

## CAUSE-EFFECT RELATIONS BETWEEN DISCHARGE CAPACITANCE AND VOLUME FORCES OF DBD PLASMA ACTUATORS

M. Kuhnhehn, B. Simon, I. Maden, S. Grundmann

Center of Smart Interfaces, Technische Universität Darmstadt, Flughafenstraße 19, 64347 Griesheim, Germany

J. Kriegseis

Institute of Fluid Mechanics, Karlsruhe Institute of Technology (KIT), Kaiserstraße 10, 76131 Karlsruhe, Germany

### INTRODUCTION

Dielectric barrier discharge (DBD) plasma actuators are used for flow control in gas flows. Besides time-averaged investigations of the resulting volume force distribution [5] the determination of the time- and phase-averaged volume force information became more important in the past years [1, 2, 7, 9]. Although there are several publications about the development of the volume force there is no obvious agreement about the exact behaviour. It is widely accepted that the contribution of the high voltage driving the plasma discharge is different in the positive and negative half-cycles, as shown by Enloe et al. [3] and Orlov et al. [8], for instance. The investigations mentioned above use a sinusoidal driving signal to identify the phase relation of the measured volume force. The work presented in this abstract deals with the measurement of phase-averaged volume force distribution  $f(x, y, \Phi)$  at very high frequencies  $f$  of the operating voltage  $V$ , pushing the measurement technique particle image velocimetry (PIV) to its limits. For the first time the measured volume forces are assigned to the instantaneous capacity of the plasma actuator using the Lissajous figure (cyclogram), rather than the commonly used voltage signal; see Figure 1. As such, a deeper insight into the interrelation of the discharge and the resulting momentum transfer is provided.

### SETUP AND RESULTS

The velocity information was obtained by means of particle image velocimetry. The measurements were performed in quiescent air to eliminate the influence of an external flow on the wall jet generated by the plasma actuator. A single plasma actuator was driven by a high voltage sinusoidal signal with  $V_{pp} = 12$  kV and a frequency of  $f = 10$  kHz. The operating voltage was generated using a Minipuls 6 and *di-ethyl-hexyl-sebacat* (DEHS) was used for tracing. With the experimental equipment it is allowed to record up to eight phase positions at arbitrary phase angles for the chosen parameter settings of the actuator. The measured operating voltage  $V$  and charge values  $Q$  are plotted against each other in Q-V-cyclograms, also known as Lissajous figures [6]. Within the Lissajous figure the instantaneous capacitance of the actuator can be identified by calculating its slope according to

$$C(t) = \frac{dQ(t)}{dV(t)}. \quad (1)$$

Figure 1 shows the Lissajous figure of a DBD with the characteristic capacitances  $C_0$  and  $C_{eff}$ .  $C_0$  represents the electrical pure passive component (cold) capacitance and  $C_{eff}$  the ef-

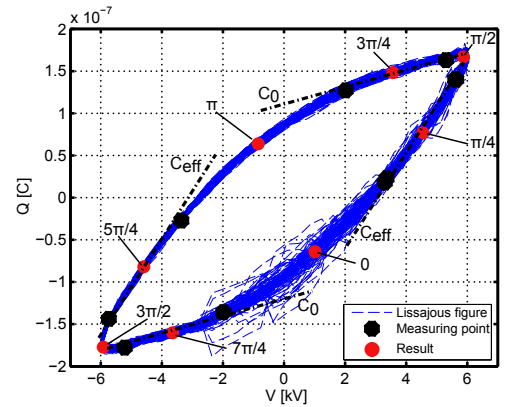


Figure 1: Typical Q-V-cyclogram (Lissajous figure) of a DBD with characteristic capacitances  $C_0$  and  $C_{eff}$ . The measuring points of the PIV measurements and the result of the correlation are emphasized.

fective capacitance, consisting of a combination of the passive component  $C_0$  and the contribution of the plasma itself to the capacitance [4]. The measurement positions for the PIV images and the resulting position of the correlated values are also shown in Figure 1. The positions were deliberately chosen to make sure that noisy areas (e. g. quenching of the plasma) are omitted.

Figure 2 shows the evolution of the actuator capacitance over phase and the determined integral value of the volume

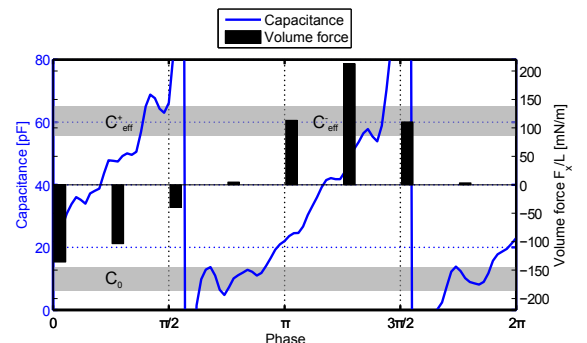


Figure 2: Evolution of the capacitance of the plasma actuator and the volume force over the measured phase positions. The characteristic capacitances  $C_0$  and  $C_{eff}$  are highlighted. The positive volume force is generated during the negative half-cycle of the sinusoidal operating voltage.

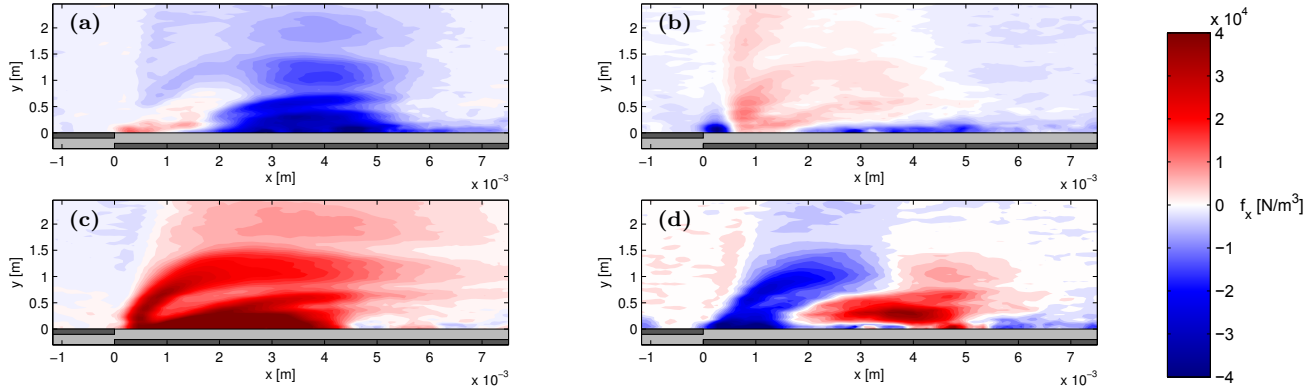


Figure 3: Spatial distribution of the volume force  $f_x$  at different phase angles.  $C_{eff}$ : (a)  $\Phi = \pi/4$ , (c)  $\Phi = 5\pi/4$ ;  $C_0$ : (b)  $\Phi = 3\pi/4$ , (d)  $\Phi = 7\pi/4$ .

force per phase. The positive volume force is generated in the negative half-cycle, during the appearance of a glow type discharge [3]. The existence of areas with almost zero volume force for two phases is remarkable ( $\Phi = 3\pi/4$  and  $\Phi = 7\pi/4$ ). In both cases the volume force is zero for the dark periods [6] with a pure passive capacitance  $C_0$  in the cyclogram, where positive and negative parts of the volume force compensate each other. The quenching of the plasma induces the deceleration of the flow and simultaneously the capacitance changes from  $C_{eff}$  to  $C_0$ , as can be identified from the shark kinks in the Lissajous figure. The spatial distribution of the volume force  $f_x$  at different phase angles is shown in Figure 3. Figures 3a and 3c correspond to the effective capacitance  $C_{eff}$  while Figures 3b and 3d refer to the passive component capacitance  $C_0$ . The positive and negative contributions to the volume force in Figure 3b and 3d compensate each other, such that the resulting volume force is approximately zero.

The resulting volume force is in good agreement with previous publications (see Figure 4). The findings of Neumann et al. [7] show almost the same development, even though measured with laser doppler anemometry (LDA). The results presented in this abstract and the results of Neumann et al. [7] show a slightly shifted behaviour due to the fact that the operating frequency is higher compared to the measurements of Benard et al. [1], Debien et al. [2] and Wilke [9]. It is hypothesized that - despite reasonable Stokes number - the higher frequencies imply a slight phase lack between the flow and the tracers.

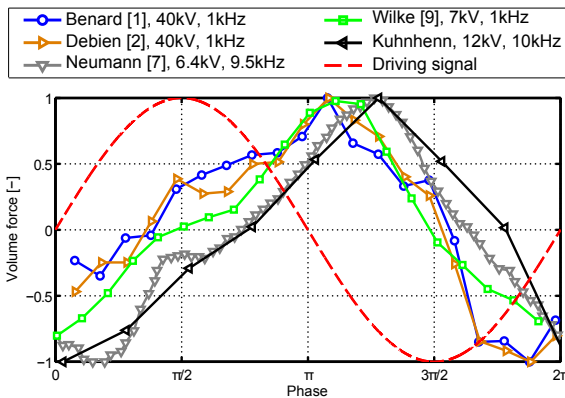


Figure 4: Evolution of the volume force compared to previous publications of Benard et al. [1], Debien et al. [2], Neumann et al. [7], Wilke [9].

## CONCLUSION

The temporal evolution and spatial distribution of the volume force at a high frequency operating voltage shows a similar behaviour compared to previous publications. In agreement with literature the results show that the positive volume force is generated in the negative half-cycle during the glow-discharge and the negative volume force is formed in the positive half-cycle during the streamer-discharge. Additional consideration of the Lissajous figure clearly uncovers the dependency of the generated volume force to rely on the instantaneous capacity of the plasma actuator rather than the operating voltage. During the dark periods, thus passive capacitance  $C_0$ , the overall volume force is counterbalanced to approximately zero. The main part of the plasma discharge at  $C_{eff}$  shows the major contribution to the resulting volume force. The streamer type discharge in the positive half-cycle is not able to compensate the dominant negative volume force, which in turn leads to a negative volume force at the respective phase. In conclusion, this new insight into the capacitance-volume force-interrelation might serve as the basis for novel control concepts in discharge-based closed-loop control applications in aerodynamics.

## REFERENCES

- [1] N. Benard, A. Debien, and E. Moreau. *Journal of Physics D: Applied Physics*, 46(245201), 2013.
- [2] A. Debien, N. Benard, L. David, and E. Moreau. *Applied Physics Letters*, 100(013901), 2012.
- [3] C. L. Enloe, M. G. McHarg, and T. E. McLaughlin. *Journal of Applied Physics*, 103(073302), 2008.
- [4] J. Kriegseis, B. Möller, S. Grundmann, and C. Tropea. *Journal of Electrostatics*, 69:302–312, 2011.
- [5] J. Kriegseis, C. Schwarz, C. Tropea, and S. Grundmann. *Journal of Physics D: Applied Physics*, 46(055202), 2013.
- [6] T. C. Manley. *J. Electrochem. Soc.*, 84(1):83–96, 1943.
- [7] M. Neumann, C. Friedrich, J. Czarske, J. Kriegseis, and S. Grundmann. *Journal of Physics D: Applied Physics*, 46(042001), 2012.
- [8] D. M. Orlov, G. I. Font, and D. Edelstein. *AIAA Journal*, 46(12):3142–3148, 2008.
- [9] J. B. Wilke. PhD thesis, Technische Universität Darmstadt, 2009.